Investigation of piezoelectric harvester performance for several shape of piezoelectric using finite element method

Nik Ahmad Kamil Zainal Abidin, Norkharziana Mohd Nayan*, Nursabirah Jamel, Azuwa Ali

Centre of Excellence for Renewable Energy (CERE), Faculty of Electrical Engineering & Technology, Universiti Malaysia Perlis, Pauh Putra Campus, 02600 Arau, Perlis, Malaysia.

Corresponding author* email: norkharziana@unimap.edu.my
Available online 30 December 2023

ABSTRACT

Energy harvesting is a prominent means of ensuring energy sustainability and among popular source to be harvest is the rainfall for the water supply and also electric from the vibration of the rain drops. Raindrop vibration is commonly harvested using piezoelectric method; hence a specific piezoelectric structure is required to properly convert vibration to electric output. Usually, a cantilever beam structure piezoelectric is used as converter element. For maximum power output, the piezoelectric cantilever beam must generate frequency vibration near at its resonant frequency. However, the cantilever beam structure has several types of shape that can generate different output at their resonant frequency. Further investigation on several geometries of piezoelectric energy harvesters is simulated using COMSOL software in order to select suitable design with maximum power generating performance. This paper present four different geometries of piezoelectric energy harvester which are basic shape, T shape, trapezoidal shape and exponential shape. The output voltage and current were investigated to obtain the optimum output based on the result of the simulation. The results indicated that the trapezoidal shape width 24mm produced the largest power which is 36.83%, 63.04 % and 78.80 % than basic shape width 16mm, T shape width 24mm and exponential shape width 32mm that generated power output at eigen frequency mode 1.

Keywords: Piezoelectric cantilever beam, Energy harvesting, Rainfall

NOMENCLATURE

m= mass

k = spring coefficient

w_n = natural frequency

ζ= damping ratio

c_p = elastic constant of the piezoelectric material

k_{31} = piezoelectric coupling coefficient

t_c = thickness of one layer of the piezoelectric material

k_2= geometric constant that relates average piezoelectric material strain to the tip deflection

ε= dielectric constant of piezoelectric material

R= load resistance

V= voltage across the load resistance

C_b= capacitance of the piezoelectric bimorph

1. Introduction

Energy harvesting is the technology of generating electricity from external source that exists in the surrounding environment, such as solar energy, wind energy, thermal energy, and vibration energy [1-4]. Vibrational energy, as a kind of widely existing energy in nature, has great potential for development and application. The rainfall vibration energy can be converted to electric energy by electromagnetic, electrostatic, piezoelectric and magnetostrictive energy harvesters [5-8]. Piezoelectric energy harvesters are the most common energy harvester when compared to other energy harvesters because of their high-power density, does not pollute the environment, wide range of frequencies, ease of miniaturisation, and integration [9-12]. As a result, piezoelectric energy harvesting research has attracted a huge interest in the last several years.

Among piezoelectric energy harvesters, the cantilever beam structure type is most popular due to great potential in powering low load devices. As a result, some researchers have attempted to improve the cantilever type's power generating performance by experimenting with various shapes. Samah Ben Ayed had investigate the effects of shape variations of a cantilever beam on its performance as an energy harvester using linear and quadratic shape. This shape was design to generate energy at low frequencies and maximize the harvested energy. The result shows the quadratic shape can yield up to two times the energy harvested by a rectangular shape [13]. Khaled Mohamed had constructed five harvester with different shapes, which are the T-shaped, rectangular, L-shaped, variable width, and triangular cantilevers. The results indicated that the T- shaped cantilever produced the largest power which is 70.71 % than triangular shape that generated the lowest power output.[14]. K.F. Wang presented work a nonlinear model of a piezoelectric harvester with various geometrical parameters which are trapezoidal, exponential, rectangular and sinusoidal beam. Therefore, designing a beam with exponentially varying shape can obtain the largest power density [5].

The structural properties of a T-shape piezoelectric cantilever beam are analysed for piezoelectric energy harvesting because of its least stiff structure. A cantilever beam is suited for this analysis to obtain the lower resonance frequency and higher stress of the energy harvester [15]. The amount of maximum stress and total elastic strain energy was found 2.39×108 N m $^{-2}$ and 0.28 mJ. Seyed akhreddin Nabavi was research about T-shaped geometry with integration of two identical proof masses at the T-segment. The research was compared between conventional straight cantilever configuration and T-shaped geometry. The result show the proposed T-shaped harvester's average power density is 4.8 times higher than the conventional one [16].

In this paper, three different geometries of piezoelectric energy harvester are investigated which are T, trapezoidal and exponential shape. The vibration source is specific to raindrops/rainfall with the output voltage and current as the components to be analysed. The finite element techniques in COMSOL Multiphysics software are used to simulate the three various geometries as they would be in actual situations. The aim to produce maximum output to power up low load application and reducing the dependency in conventional source.

2. Piezoelectric Background

Piezoelectric materials exhibit both electric and mechanical behaviour at the same time, and thus have a wide range of applications such as sensor applications include force sensors and displacement sensors using piezoelectric effect. Linear motors and precision stages with inverse piezoelectric effect are examples of actuator uses. With dipole moments, piezoelectric element generates proportionally electric energy when mechanical energy is applied to it and vice versa. The piezoelectric constitutive equation represents the relation of stress and voltage.

$$S = s^E T + dE \quad (1)$$

$$D = dT + \varepsilon^T E \quad (2)$$

Where S is strain, s compliance, E electric field, T stress, D electric displacement, d piezoelectric coefficient, and ε dielectric constant. From Eqs. (1) and (2), energy conversion relation is expressed in piezoelectric coupling factors. The piezoelectric coefficient, d, represents the amount of charge generated by the relationship between stress and dipole moment. The piezoelectric coefficient is a constant value in static loading, but variable in dynamic loading such as resonant frequency [17][18].

The piezoelectric material produces electrical energy from the stress on the beam. The maximum generated power of electrical energy in energy harvesting can be affected by material properties, configuration, and load impedance.

$$P = \frac{V^{2}}{2R} = \frac{1}{2R} \times \frac{\left(\frac{2k_{31}t_c}{k_2}\right)^{2}\frac{c_p}{\varepsilon}{A_{in}}^{2}}{\left[\frac{{w_n}^{2}}{\omega RC_b} - \omega\left(\frac{1}{RC_b} + 2\zeta\omega_n\right)\right]^{2} + \left[{w_n}^{2}\left(1 + {k_{31}}^{2}\right) + \frac{2\zeta\omega_n}{RC_b} - \omega^{2}\right]^{2}} \quad (3)$$

$$P = \frac{m^{2}}{2k} \times \frac{{RC_b}^{2}\left(\frac{2k_{31}t_c}{k_2}\right)^{2}\frac{c_p}{\varepsilon}{A_{in}}^{2}}{\left(4\zeta^{2} + {k_{31}}^{4}\right)(RC_b)^{2}k + 4\zeta{k_{31}}^{2}RC_b\sqrt{km} + 4\zeta^{2}m} \quad (4)$$

Unfortunately, using the equation above, it is difficult to predict the generated power for a complicated shape [17]. In order to produce more efficient results, the generated voltage from the piezoelectric material should be analysed using a commercial finite element method (FEM) tool for more complicated model as compared to the basic model. For this reason, COMSOL Multiphysics software was used to analyse basic parameters in the experiments.

2.1 Simulation using COMSOL

The designed 3-D model was done in COMSOL Multiphysics in order to analysis its mechanical and electrical properties. In solid mechanics physics, the boundary condition for the beam such as free end, fixed end, applied force vibration and damping of the beam materials have been set up. The base part of the beam was kept constant. The rest of the beam was under free conditions. After applying vibration the free part can be displaced. Mechanical damping for both PVDF and silver layers was set 0.001. The applied force vibration sources for the beam was kept 3.1 N. During the boundary conditions of electrostatics physics, the top and bottom surface of the piezoelectric layers was used as terminal and ground. The electrostatics physics was coupled with electrical circuit physics so that electrical response of the beam can be obtained. Table 1 show material Properties of the PVDF Cantilever.

Table 1. Material Properties of the PVDF Cantilever

Properties	**Material PVDF**
Young's modulus (10^9 N/m^2)	2-4
Poisson's ratio	0.34
Density (kg/m)	1780

After that, tetrahedral mesh with fine element size were used for the discretization of the beam. Eigen frequency analysis was performed to determine eigenvalue of the beam. Finally, first mode eigen frequency analyses were conducted for the cantilever beam and they are frequency dependence and load dependence.

3. Simulated Structures

COMSOL Multiphysics software is utilized to simulate the behaviour and characteristics of the piezoelectric transducer under impact pressure, applied on the surface of the piezoelectric. The dimensions of the transducer were optimized to generate the maximum voltage. The transducer consisted of two types of materials, namely PVDF and sandwiched between two silver layers as electrodes. There are three types of shape was study which are T shape, trapezoidal shape and exponential shape with difference width. The piezoelectric structures and simulation parameters are shown in table 2 and table 3 respectively. In this experiment, the impact of load is applied on the free end of cantilever transducer because the impact on the free end generated higher voltage than impacting on the centre [19].

After that, tetrahedral mesh with fine element size were used for the discretization of the beam. The eigenfrequency analysis is used to determine a structure's natural frequencies and associated mode shapes. Table 3 shows the values of the frequency modes and their associated deformation shapes. The cantilever's bending behaviour is suited for the energy

harvester application, therefore mode 1 frequency is chosen as its resonance frequency [20]. Finally, first mode eigen frequency analyses were conducted for the cantilever beam and they are frequency dependence and load dependence.

Table 2. Simulation parameters of piezoelectric

Shape	Length (mm)	Width (mm)	Thickness (mm)
T shape	41	24,32,48	0.04
Exponential shape	41	24,32,48	0.04
Trapezoidal shape	41	24,32,48	0.04

Table 3. Schematic diagram of piezoelectric PVDF T shape Exponential shape and Trapezoidal shape.

T shape	Exponential shape	Trapezoidal shape
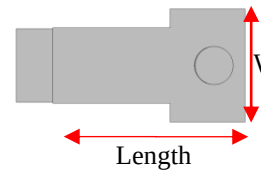	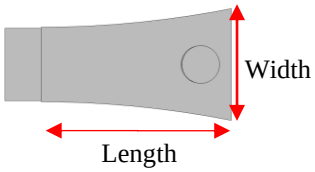	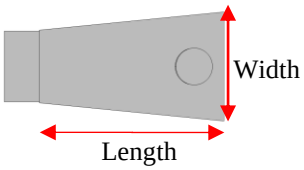
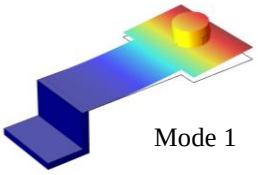	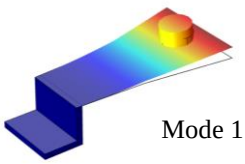	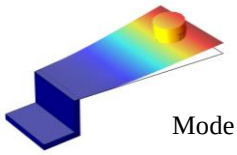
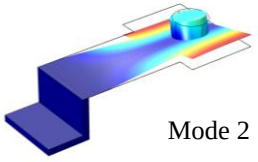	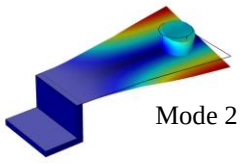	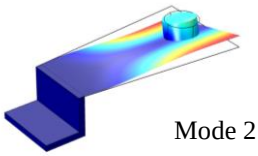
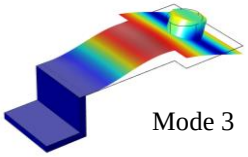	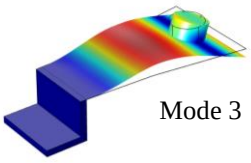	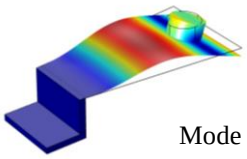

The typical raindrop diameter from an actual rain event ranges from 0.01 mm to 5.8 mm. In this study, the sizes of droplet diameter is 4.5 mm with 3.1 N impact force are selected based on previous research result. The output voltage and power are analysed to find the best shape of piezoelectric [21].

4. Results and Discussions

The modal analysis is initially investigated using a variety of shapes. The modal analysis is carried out in order to determine the cantilever beams eigenfrequencies in each mode. The modal analysis results are presented in table 3, and the voltage output results of the Basic shape with a width of 16 mm across 10 MΩ resistive loads are shown in figure 1

(a). The results indicate that at eigenfrequency mode 1, the output voltage was 37.94V, while at mode 3, it was 0.88 V. However, there was no voltage output (0V) at mode 2 eigenfrequency. These measurements were taken while maintaining a fixed pre-stress condition of 3.1 N and varying the load resistance. Notably, the basic shape with a width of 16 mm can deliver a maximum output power of about 0.07 mW at the eigenfrequency of 3.1882 Hz when connected to a 10 MΩ resistive load.

Table 4. Modal analysis of T shape width 16 mm

Mode	Eigen frequency (Hz)	Width (mm)
1	3.1882	
2	28.485	Basic shape
3	52.651	

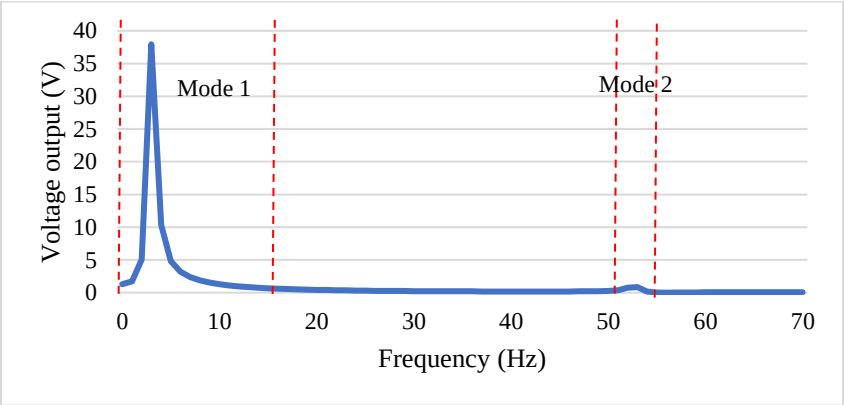

(a)

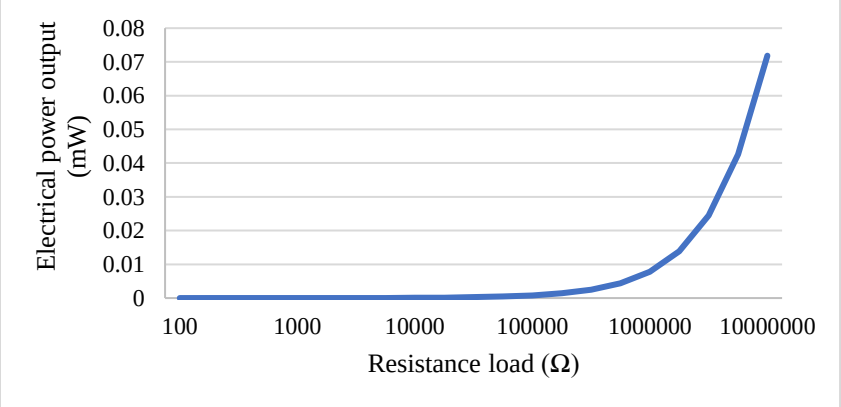

(b)

Figure. 1. Voltage output (a) and power (b) of Basic shape width 16mm

Modal analysis results presented in table 5. Figure 2 (a) shows the voltage output results of T shape with width 24mm through 10 MΩ resistive loads. The result show at eigenfrequency mode 1 the output voltage was 36V and mode 3 the output voltage was 2V. However, at mode 2 eigenfrequency the voltage output at 0V. The results were measured as a function of load resistance with a fixed pre-stress condition (3.1 N). A maximal output power of about 0.068 mW can be obtained from the T shape width 24mm at the eigenfrequency of 3.1886 Hz across a resistive load of 10 MΩ.

Table 5. Modal analysis of T shape width 24 mm

Mode	Eigen frequency (Hz)	Width (mm)
1	3.1886	
2	28.625	T shape
3	60.868	

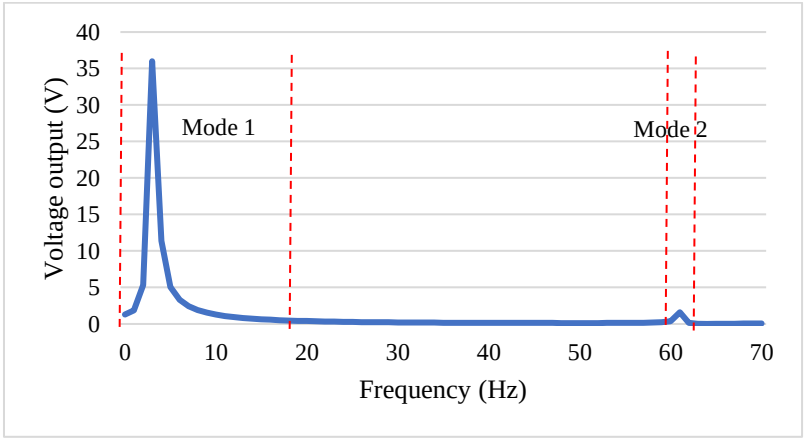

(a)

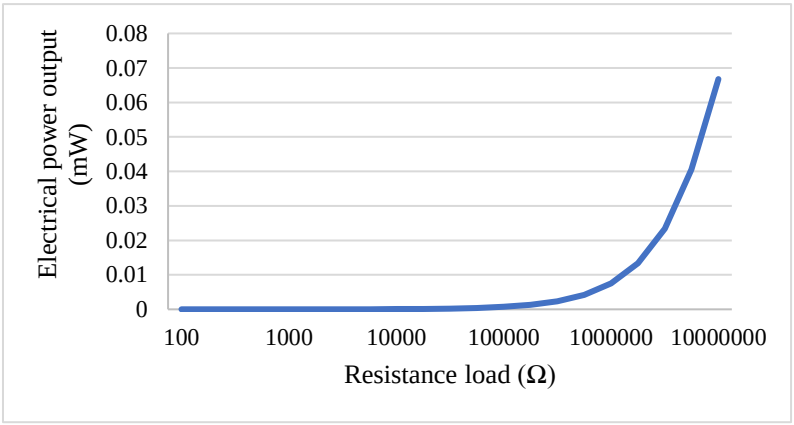

(b)

Figure. 2. Voltage output (a) and power (b) of T shape width 24mm

Modal analysis results are in table 6. The highest output voltage and output of T shape with width 32mm power are shown in figures 3(a) and (b). The result shows, a maximal output power of 0.024 mW can be obtained from the T shape width 32mm at 2.7808 Hz through a resistive load of 10 MΩ while the voltage of 21.8 V at mode 1 and mode 3 the output voltage was 0.9V can be generated under a fixed pre-stress condition (3.1 N). However, at mode 2 eigenfrequency the voltage output at 0V.

Table 6. Modal analysis of T shape width 32 mm

Mode	Eigen frequency (Hz)	Width (mm)
1	2.7808	
2	25.639	T shape
3	61.538	

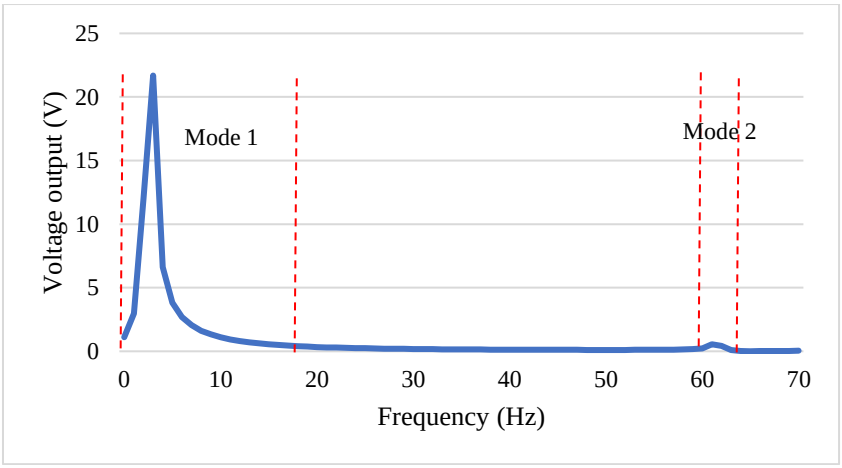

(a)

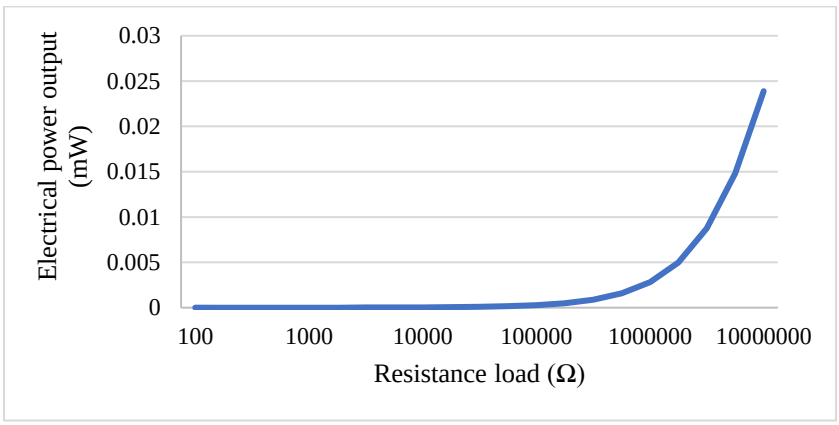

(b)

Figure. 3. Voltage output (a) and power (b) of T shape width 32mm

Figure 4(a) and (b) shown the maximum of the output voltage and the output power of T shape with width 48mm under a fixed pre-stress condition (3.1 N), meantime, the eigenfrequency of the harvester is shown in table 7. The result shows, a maximal output power of 0.265 mW can be obtained from the T shape with width 48mm through a resistive load of 10 MΩ while the maximum output voltage of 26.4 V at mode 1 and mode 3 the output voltage was 1.8V. However, at mode 2 eigenfrequency the voltage output at 0V.

Table 7. Modal analysis of T shape width 48 mm

Mode	Eigen frequency (Hz)	Width (mm)
1	2.2814	
2	19.298	T shape
3	62.991	

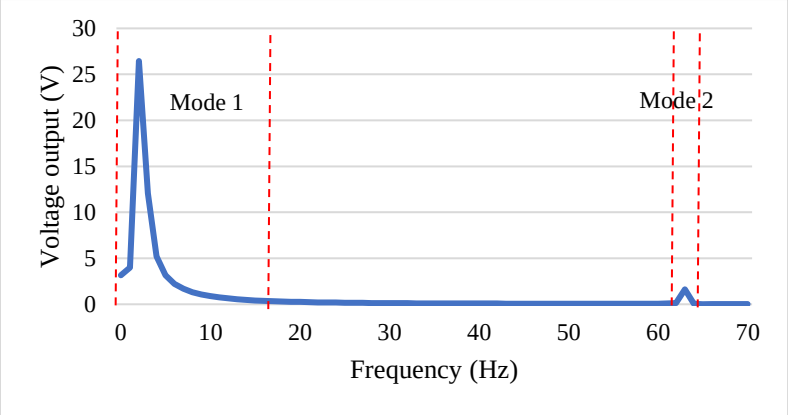

(a)

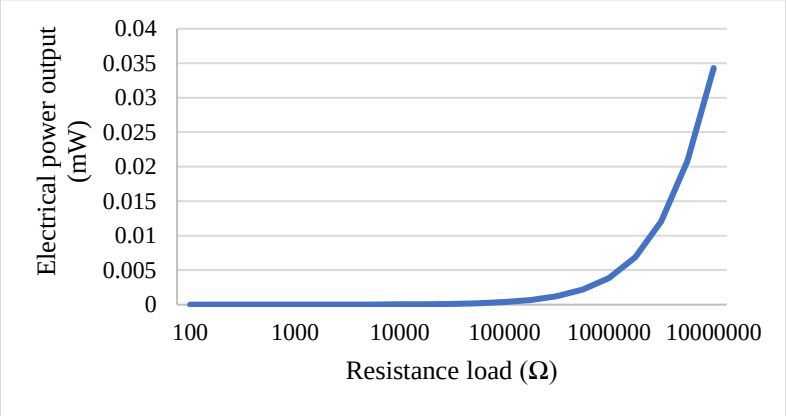

(b)

Figure. 4. Voltage output (a) and power (b) of T shape width 48mm

Figure 5(a) shown that the output voltage at their eigenfrequency modes that show in table 8 using exponential shape with width 24mm. When the eigenfrequency is at mode 1 the maximum voltage approaches 15.9 V and at mode 3 the output voltage is 2.8 V. Fig. 6(b) shows that a maximum output power of about 0.012 mW generated with resistive load 10 MΩ. However, at mode 2 eigenfrequency the voltage output at 0V.

Table 8. Modal analysis of exponential shape width 24 mm

Mode	Eigen frequency (Hz)	Width (mm)
1	3.4606	
2	30.817	Exponential
3	65.780	

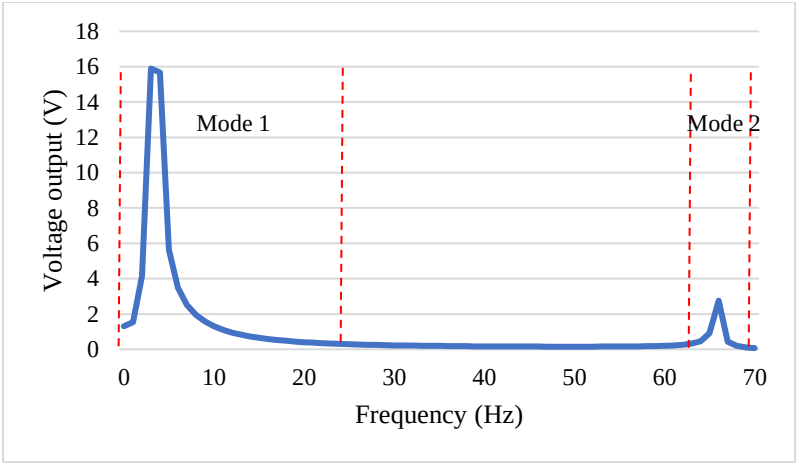

(a)

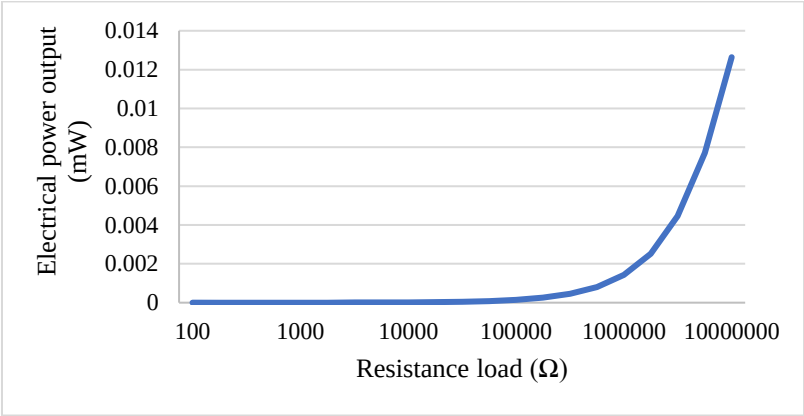

(b)

Figure. 5. Voltage output (a) and power (b) of exponential shape width 24mm

Modal analysis results are in table 9. Based on the results in figure 6(a), the maximum voltage of 28 V was generated when eigenfrequency at mode 1 and at mode 3 the generated output voltage was 1.8 V using exponential shape with width 32mm. The maximum output power shown in figure 6(b) of about 0.039 mW generated with resistive load 10 MΩ. However, at mode 2 eigenfrequency the voltage output at 0V.

Table 9. Modal analysis of exponential shape width 32 mm

Mode	Eigen frequency (Hz)	Width (mm)
1	3.2478	
2	26.828	Exponential
3	56.353	

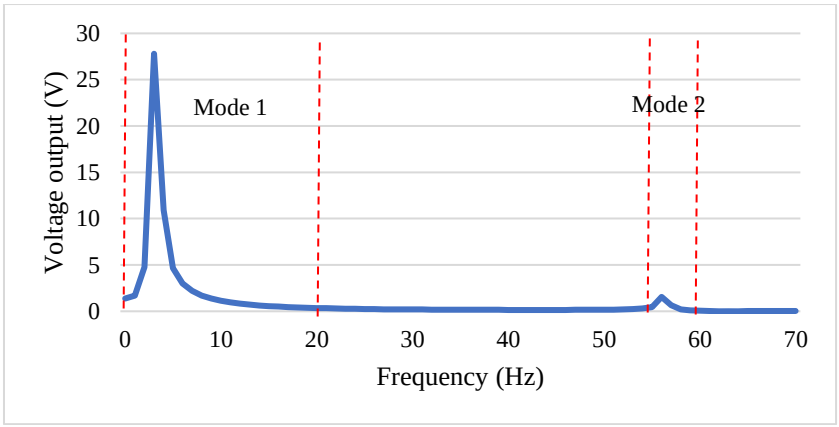

(a)

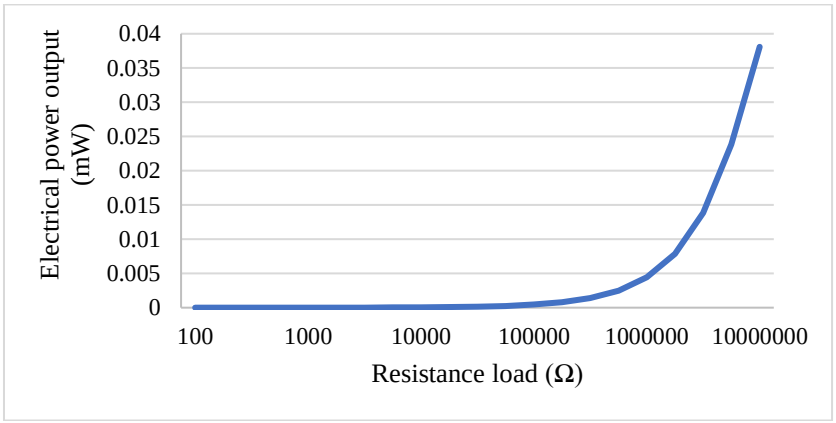

(b)

Figure. 6. Voltage output (a) and power (b) of exponential shape width 32mm

As shown in figure 7(a) and (b), a maximal output power of 0.035 mW can be obtained from the of exponential shape with width 48mm at mode 1 eigenfrequency through a resistive load of 10 MΩ, while the maximum voltage of 26 V can be generated at mode 1 eigenfrequency and at mode 3 the generated output voltage was 1.5 V. However, at mode 2 eigenfrequency the voltage output at 0V. Modal analysis results are in table 10.

Table 10. Modal analysis of exponential shape width 48 mm

Mode	Eigen frequency (Hz)	Width (mm)
1	3.6448	
2	27.616	Exponential
3	69.641	

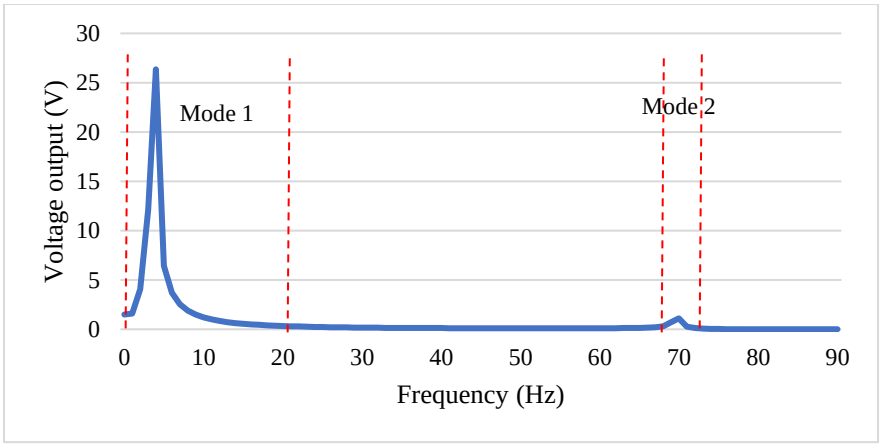

(a)

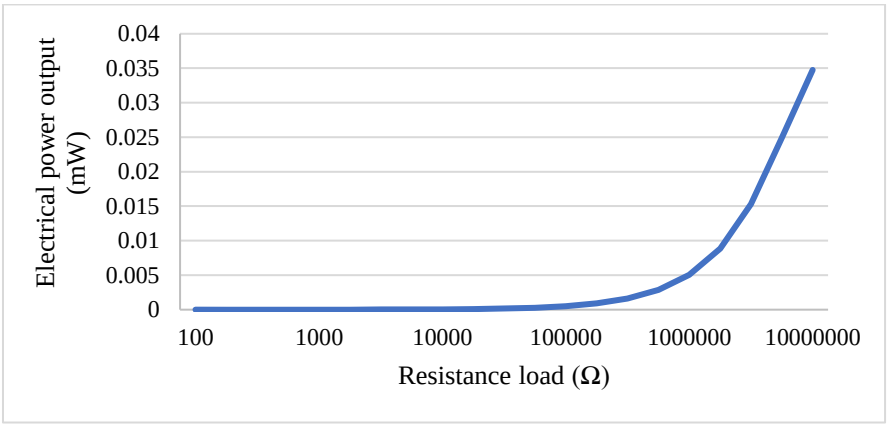

(b)

Figure. 7. Voltage output (a) and power (b) of exponential shape width 48mm

Figure 8(a) and (b) shown the maximum of the output voltage and the output power of trapezoidal shape with width 24mm under a fixed pre-stress condition (3.1 N), meantime, the eigenfrequency of the harvester is shown in table 11. The result shows, a maximal output power of 0.184 mW can be obtained from the trapezoidal shape with width 24mm through a resistive load of 10 MΩ while the maximum output voltage of 60 V at mode 1 and mode 3 the output voltage was 0.1V. However, at mode 2 eigenfrequency the voltage output at 0V.

Table 11. Modal analysis of trapezoidal shape width 24mm

Mode	Eigen frequency (Hz)	Width (mm)
1	3.1406	
2	27.734	Trapezoidal
3	55.609	

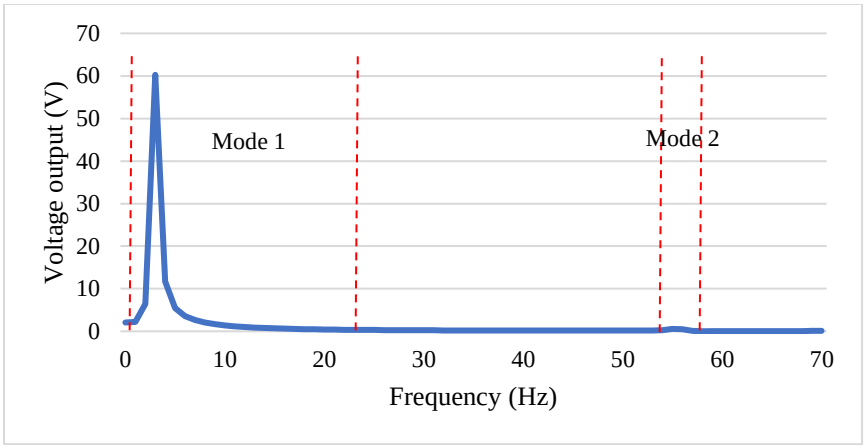

(a)

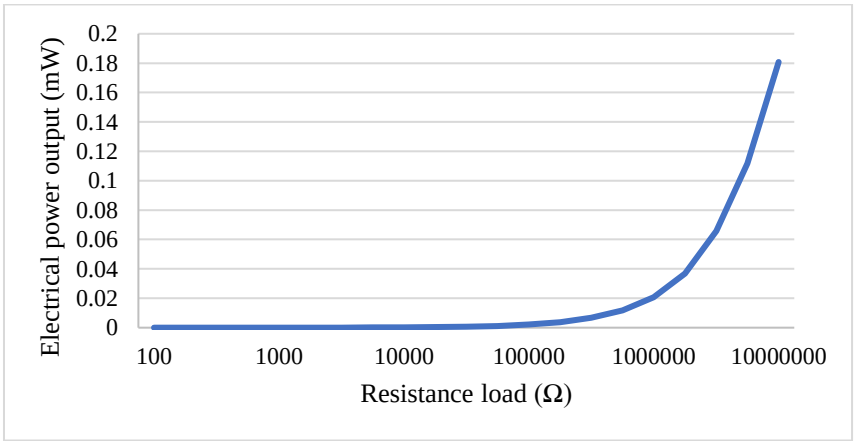

(b)

Figure. 8. Voltage output (a) and power (b) of trapezoidal shape width 24mm

Modal analysis results are in table 12. Based on the results in figure 9(a), the maximum voltage of 11.9 V was generated when eigenfrequency at mode 1, and at mode 2 and 3 the generated output voltage was 0.5 V and 1.8 V using trapezoidal shape with width 32mm. The maximum output power shown in figure 10(b) of about 0.007 mW generated with resistive load 10 MΩ.

Table 12. Modal analysis of trapezoidal shape width 32mm

Mode	Eigen frequency (Hz)	Width (mm)
1	6.2087	
2	51.466	Trapezoidal
3	222.84	

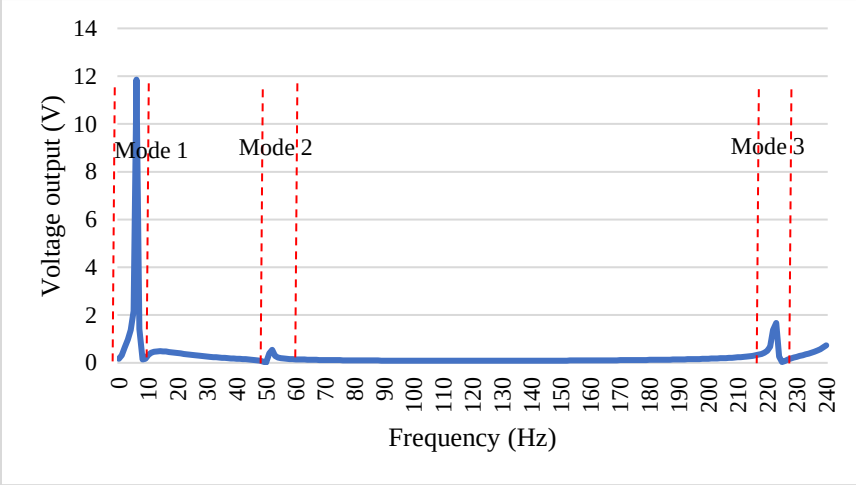

(a)

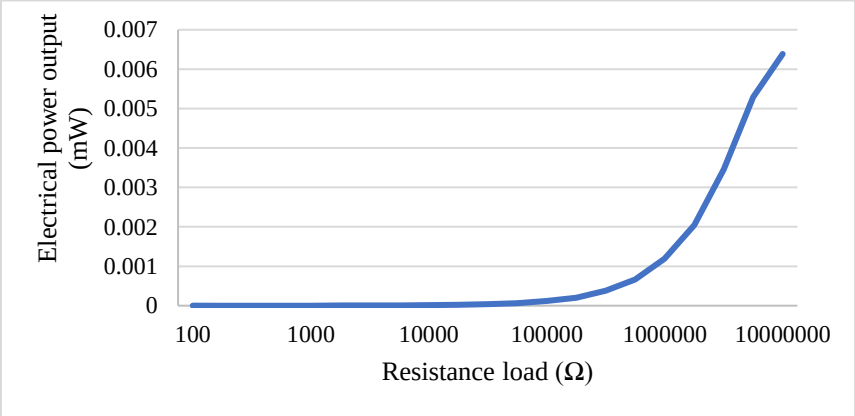

(b)

Figure. 9. Voltage output (a) and power (b) of trapezoidal shape width 32mm

Figure 10(a) shown that the output voltage at their eigenfrequency modes that show in table 13 using trapezoidal shape with width 48mm. When the eigenfrequency is at mode 1 the maximum voltage approaches 5.3 V and at mode 3 the output voltage is 0.39 V. Figure 10(b) shows that a maximum output power of about 0.001 mW generated with resistive load 10 MΩ. However, at mode 2 eigenfrequency the voltage output at 0V.

Table 13. Modal analysis of trapezoidal shape width 48mm

Mode	Eigen frequency (Hz)	Width (mm)
1	0.001	
2	22.787	Trapezoidal
3	59.936	

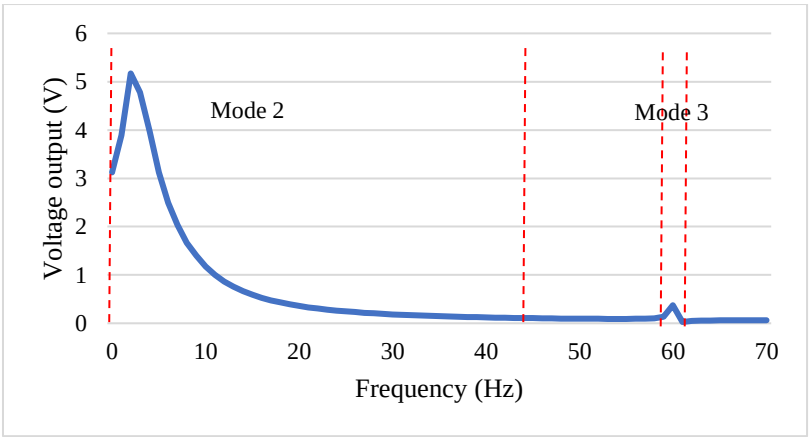

(a)

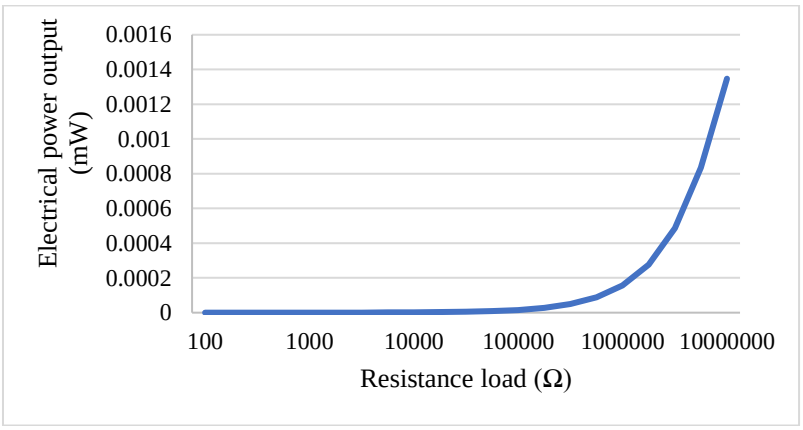

(b)

Figure. 10. Voltage output (a) and power (b) of trapezoidal shape width 48mm

Figure 11 shows the COMSOL simulation results for the various ten shapes of cantilever beam. The natural frequency and deflection of the three forms were determined using the Eigen frequency research. In table 14, the eigen frequencies, output power, electric voltage and resistive load of the different forms were estimated and summarised. Table 13 shows that the trapezoidal shape width 24mm construction produce the most output of voltage and power. The results indicated that the trapezoidal shape width 24mm produced the largest power which is 36.83%, 63.04 % and 78.80 % than basic shape width 16mm, T shape width 24mm and exponential shape width 32mm that generated power output at eigen frequency mode 1.

Table 14. Summary Eigen frequency, voltage, power output and resisting load

Cantilever shape	**Eigen frequency (Hz) mode 1**	**Output power (mW) at 10 MΩ**	**Output voltage (V) at 10 MΩ**
Basic shape width 16mm	3.1882	0.07	37.9
T shape width 24mm	3.1886	0.068	36
T shape width 32mm	2.7808	0.024	21.8
T shape width 48mm	2.2814	0.034	26.4
Exponential shape width 24mm	3.4606	0.012	15.9
Exponential shape width 32mm	3.2478	0.039	28
Exponential shape width 48mm	3.6448	0.035	26
Trapezoidal shape width 24mm	3.1406	0.184	60
Trapezoidal shape width 32mm	6.2087	0.007	11.9
Trapezoidal shape width 48mm	0.001	0.001	5.3

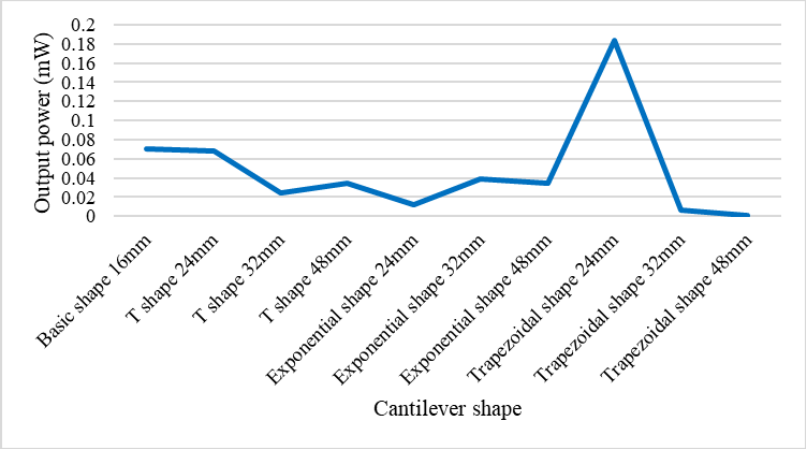

Figure. 11. Output power of cantilever shapes.

5. Conclusions

In this study, to obtain the optimum power output from several types of shape piezoelectric energy harvester, piezoelectric cantilever is designed based on finite element method. The finite element analysis comsol software is used to simulate the relationship between the shape and the natural frequencies of the piezoelectric cantilever. The three types of shape piezoelectric energy harvester with different width was investigate which are T shape, trapezoidal shape and exponential shape are designed using simulation results. Results show that the highest output power among four types of shape piezoelectric energy harvester with different width show trapezoidal shape width 24mm generated 0.184 mW with resistive load 10 MΩ at 2.8249 Hz. Another three types of shape piezoelectric which are basic shape with width 16mm generated 0.07 mW with resistive load 10 MΩ at 3.1882Hz, T shape with width 24mm generated 0.068 mW with resistive load 10 MΩ at 3.1886 Hz and exponential shape with width 32mm generated 0.039 mW with resistive load 10 MΩ at 3.2478Hz. the. The results indicated that the trapezoidal shape width 24mm produced the largest power which is 36.83%, 63.04 % and 78.80 % than basic shape width 16mm, T shape width 24mm and exponential shape width 32mm that generated power output at eigen frequency mode 1.

Acknowledgment

The authors would like to acknowledge the support from Fundamental Research Grant Scheme (FRGS/1/2018/TK04/UniMAP/02/5) from Ministry of Higher Learning Malaysia and Universiti Malaysia Perlis (UniMAP) and for providing research facilities.

5. References

[1] A. Khalid, A. K. Redhewal, M. Kumar, and A. Srivastav, “Piezoelectric Vibration Harvesters Based on Vibrations of Cantilevered Bimorphs: A Review,” *Mater. Sci. Appl.*, vol. 06, no. 09, pp. 818–827, 2015.

[2] N. A. K. Z. Abidin, N. M. Nayan, M. M. Azizan, and A. Ali, “Analysis of voltage multiplier circuit simulation for rain energy harvesting using circular piezoelectric,” *Mech. Syst. Signal Process.*, vol. 101, pp. 211–218, 2018.

[3] S. Materials, A. Engineering, and H. Kong, “On the Influence of Transducer Internal Loss in Piezoelectric Energy Harvesting with SSHI Interface,” vol. 22, no. March, pp. 503–512, 2011.

[4] N. Ahmad *et al.*, “Analysis of AC-DC converter circuit performance with difference piezoelectric transducer array connection,” vol. 14, no. 2, pp. 1–8, 2019.

[5] K. F. Wang, B. L. Wang, Y. Gao, and J. Y. Zhou, “Nonlinear analysis of piezoelectric wind energy harvesters with different geometrical shapes,” *Arch. Appl. Mech.*, vol. 90, no. 4, pp. 721–736, 2020.

[6] F. G. Yuan, “Designing a Battery-Less Piezoelectric based Energy Harvesting Interface Circuit with 300 mV Startup Voltage,” *J. Phys. Conf. Ser.*, vol. 431, p. 012025, 2013.

[7] N. Zhou, S. Gao, R. Li, H. Ao, and H. Jiang, “Transient output performance of symmetrical V-shaped micro-piezoelectric energy harvester by using PZT-5H,” *Microsyst. Technol.*, vol. 27, no. 3, pp. 779–787, 2021.

[8] M. G. Kang, W. S. Jung, C. Y. Kang, and S. J. Yoon, “Recent Progress on PZT Based Piezoelectric Energy Harvesting Technologies,” *Actuators*, vol. 5, no. 1, p. 5, 2016.

[9] T. Oh, S. K. Islam, G. To, and M. Mahfouz, “Powering wearable sensors with a low-power CMOS piezoelectric energy harvesting circuit,” *2017 IEEE Int. Symp. Med. Meas. Appl. MeMeA 2017 - Proc.*, pp. 308–313, 2017.

[10] J. Song, G. Zhao, B. Li, and J. Wang, "Design optimization of PVDF-based piezoelectric energy harvesters," *Heliyon*, vol. 3, no. 9, 2017.
[11] S. Saxena, R. Kumar, and V. Khare, "Materials Today : Proceedings Tuning of a wide range of low resonance frequencies by a novel multi-resonant piezoelectric energy harvester," *Mater. Today Proc.*, vol. 28, pp. 85–87, 2020.
[12] H. Liu, J. Zhong, C. Lee, S. W. Lee, and L. Lin, "A comprehensive review on piezoelectric energy harvesting technology: Materials, mechanisms, and applications," *Appl. Phys. Rev.*, vol. 5, no. 4, p. 041306, 2018.
[13] S. Ben Ayed, A. Abdelkefi, F. Najar, and M. R. Hajj, "Design and performance of variable-shaped piezoelectric energy harvesters," *J. Intell. Mater. Syst. Struct.*, vol. 25, no. 2, pp. 174–186, 2014.
[14] K. Mohamed, H. Elgamal, and S. A. Kouritem, "An experimental validation of a new shape optimization technique for piezoelectric harvesting cantilever beams," *Alexandria Eng. J.*, vol. 60, no. 1, pp. 1751–1766, 2020.
[15] M. N. Uddin, M. S. Islam, J. Sampe, S. A. Wahab, and S. H. Md Ali, "Vibration based T-shaped piezoelectric cantilever beam design using finite element method for energy harvesting devices," *IEEE Int. Conf. Semicond. Electron. Proceedings, ICSE*, no. 1, pp. 137–140, 2016.
[16] S. Nabavi, "T-Shaped Piezoelectric Structure for High-Performance MEMS Vibration Energy Harvesting," *J. Microelectromechanical Syst.*, vol. 28, no. 6, pp. 1100–1112, 2019.
[17] J. Lee and B. Choi, "A Study on the Piezoelectric Energy Conversion System using Motor Vibration," vol. 13, no. 4, pp. 573–579, 2012.
[18] E. S. Leland, J. Baker, E. Reilly, B. Otis, J. M. Rabaey, and P. K. Wright, "Improving power output for vibration-based energy scavengers," *IEEE Pervasive Comput.*, vol. 4, no. 1, pp. 28–36, 2005.
[19] M. A. Ilyas and J. Swingler, "Towards a prototype module for piezoelectric energy harvesting from raindrop impacts," *Energy*, vol. 125, pp. 716–725, 2017.
[20] U. M. Jamain, N. H. Ibrahim, and R. A. Rahim, "Performance Analysis of Zinc Oxide Piezoelectric MEMS Energy Harvester," *2014 IEEE Int. Conf. Semicond. Electron.*, pp. 263–266, 2014.
[21] C. H. Y. Yu, "Experimental determination of forces applied by liquid water drops at high drop velocities impacting a glass plate with and without a shallow water layer using wavelet deconvolution," *Exp. Fluids*, pp. 1–23, 2018.